Available online at www.sciencedirect.com

ScienceDirect

Mendeleev Commun., 2022, **32**, 467–470

Mendeleev Communications

DFT modeling of indoline spiropyrans with a cationic substituent in the gas phase

Vitaliy V. Koval,*[a] Anastasia S. Kozlenko,[a] Vladimir I. Minkin,[a] Islam M. El-Sewify[a,b] and Boris S. Lukyanov[a]

[a] *Institute of Physical and Organic Chemistry, Southern Federal University, 344090 Rostov-on-Don, Russian Federation. E-mail: vitvkoval@sfedu.ru*

[b] *Department of Chemistry, Faculty of Science, Ain Shams University, Abbassia 11566, Cairo, Egypt*

DOI: 10.1016/j.mencom.2022.07.013

Isomeric forms of indoline spiropyrans show unusual behavior compared with similar compounds, according to experimental data. DFT modeling for gas phase was made to consider the simplest case without environmental effects, which revealed the intramolecular reasons for occurrence of ring opening reaction depending on the particular structure of the compound. The questions of charge redistributions, the changes of geometry and chemical bonds in the structures are also discussed.

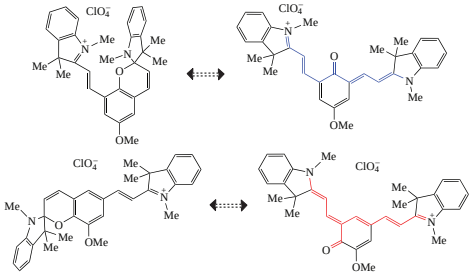

Keywords: chemical bonds, density functional calculations, merocyanine, NBO theory, spiropyrans, indolines.

Spiropyrans of indoline series are the promising building blocks to create smart materials[1] and molecular machines[2] and for application in photopharmacology.[3,4] The activity of these spiropyrans is connected with the strained C_{spiro}–O bond which is predisposed to cleavage. The isomerization includes at least two stages: the transition from closed spirocyclic (SP) form to short-lived opened *cis*-merocyanine (MC) form with C_{spiro}–O bond opening and further planarization into one of the more stable highly conjugated *trans*-MC isomers.[5–7] The reversible spirocycle rupture process can be initiated by electromagnetic irradiation or the influence of chemical species.[8] The mutual stability of SP and MC forms can be significantly different depending on the nature of substituents in the molecules.[9,10]

Spiropyrans containing a conjugated cationic fragment in the 2*H*-chromene fragment are especially interesting objects both due to their spectral and kinetic properties[10] and from the viewpoint of the formation reaction peculiarities.[11] Previously, the influence of the mutual arrangement of the cationic and anionic fragments was studied in order to establish the effect of the substituents position in the 2*H*-chromene moiety on the change in the energy of the corresponding isomers.[12] In the present study, the reversible spirocyclic rupture process has been computationally modeled in the gas phase. It allowed us to examine intramolecular factors in the computer model of isomeric reactions, excluding the influences of solution and solid-state effects. Moreover, there are examples of the good agreement between calculations in the gas phase and experimentally observed values when the described properties do not directly depend on the characteristics of the solvent.[13] The objects for modeling are isomeric structures of relative compounds **1** and **2** because their SP and MC forms have different mutual stability (Scheme 1). According to experimental data, there is SP form (**1a**) of spiropyran **1** in the DMSO solution and in solid state, while compound **2** forms the mixture of SP (**2a**) and one of the MC (**2c**,**d**) isomers in DMSO, and in crystals it exists in one of possible *trans*-MC (**2d**) forms.[14] It allowed to consider the process of opening and closing pyran ring for two compounds with similar structural motifs but different behavior of this ring.

The simulation was performed with Gaussian 16 software package.[15] The density functional theory (DFT) method with three-parameter Lee–Yang–Parr correlation functional (B3LYP)[16] and the 6-311++G(d,p) basis set[17] were used. Previously obtained XRD data[14] were used as initial geometric approximations. Stationary points on the potential energy surfaces (PES) were identified by analytical calculating the matrix of constants. The analysis of the natural bond orbitals was performed with NBO 6.0 package.[18] Optimized structures were rendered using Chemcraft program.[19] GaussView program[20] was used to visualize the electrostatic potential (ESP) map.

For considered structures the modeling approach without transition states is used due to well-known problems of DFT modeling for big size molecules such as computational complexity. So, available XRD data is starting point for modeling of **1a** and **2d**. Other structures were simulated based on reaction schemes previously proposed.[5,13,21,22] Also, the analysis of the relative positions of the natural bond orbitals in **1a**–**d** and **2a**–**d** was used for checking the results.

The NBO energetic (deletions) analysis allowed us to estimate the stabilizing effect of the localized and delocalized (non-Lewis) contributions in the structural stability. The Lewis-type wavefunction of structure has an energy E(L) greater the full energy E(full). The value of E(L) allows one to estimate localized contribution in structural stability. Also, the net energy difference E(NL) = E(full) – E(L) enables to estimate the stabilizing effect of the delocalizing (non-Lewis) contributions.

The relative values of E(L) and E(NL) for isomeric structures of compounds **1** and **2** are shown in Figure 1. The summary of

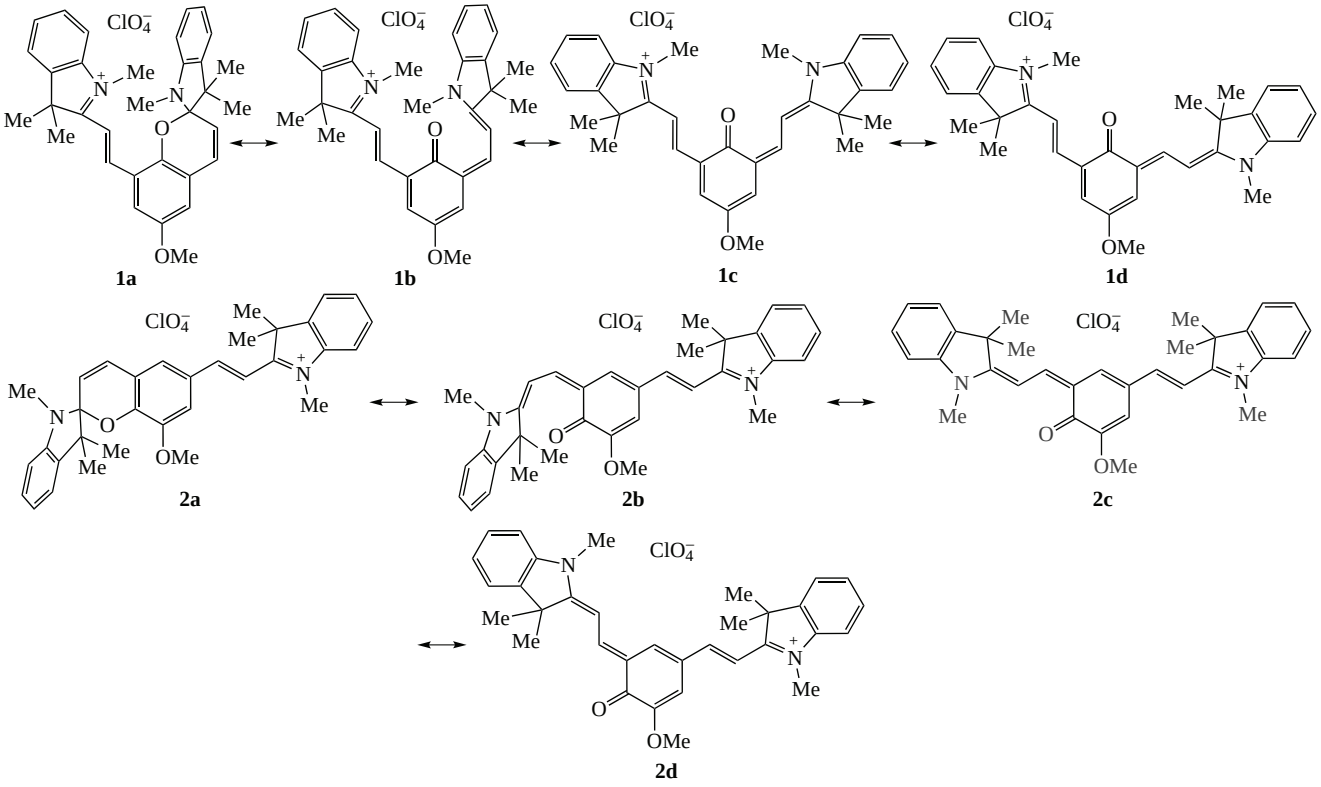

Scheme 1

deletions analysis is outlined in Table S4 (see Online Supplementary Materials). The stability of **1a**, **1c** and **1d** has been favored by localized contribution, whereas the stability of **1b** can be attributed to the electronic delocalization energy *E*(NL). However, the large differences in Δ*E*(L) values for **1a** and **1b** and for **1b** and **1c** cast doubt on the possibility of the corresponding isomerization reactions.

The consideration of structures **1a′**–**d′** without perchlorate anion allowed us to reveal the anion effect on the cationic fragment in part of *E*(L) and *E*(NL) energies. However, preserving the rather large difference in Δ*E*(L) values for **1a′** and **1b′** suggests that the pyran ring opening is not possible under normal conditions for cation case also. In other words, the pyran ring preservation is a property of the cationic part of compound **1** itself due to disbalance between localized and delocalized contributions in the structural stability in favor of localized one.

All four considered isomeric structures of compound **2** are characterized by *E*(L) and *E*(NL) values of a similar order. So,

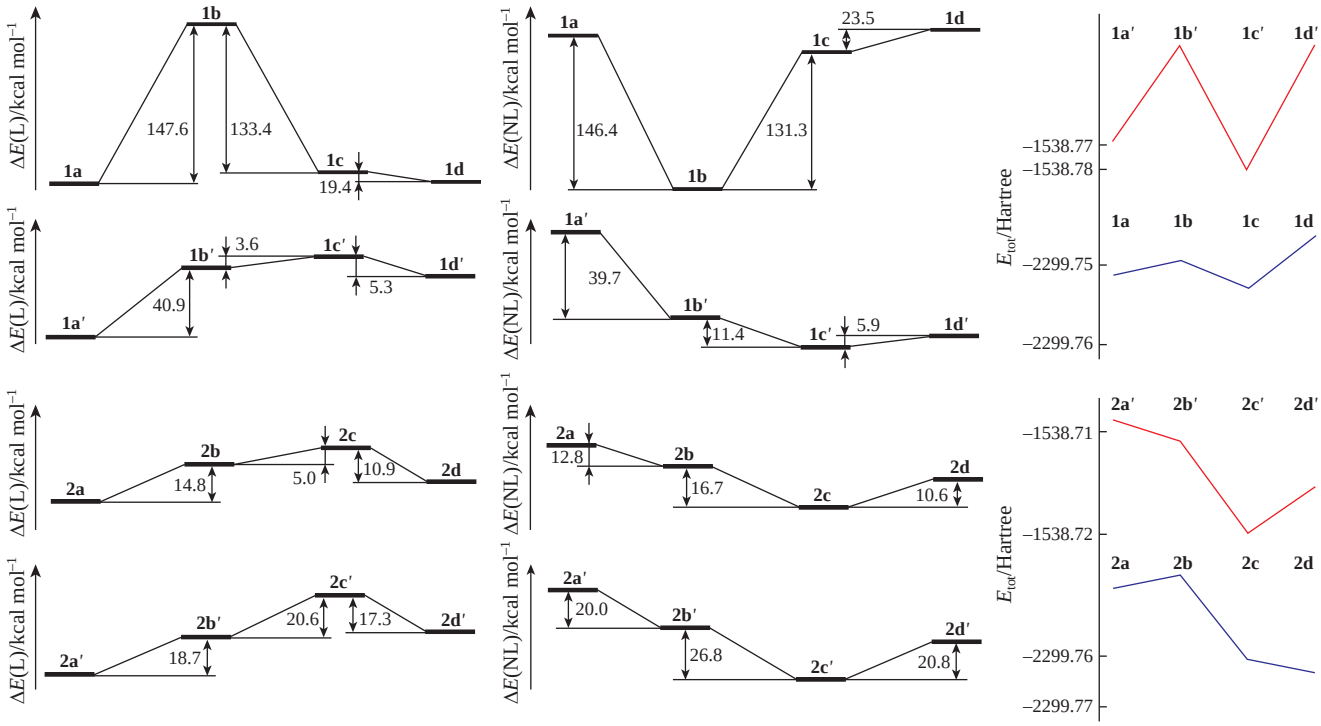

Figure 1 The schematic energy profiles of the Lewis-type wavefunction energy *E*(L) and the net energy difference *E*(NL), and the graphics of total electronic energy E_{tot} for isomeric structures with (**1a**–**d**, **2a**–**d**) and without (**1a′**–**d′**, **2a′**–**d′**) perchlorate anion.

all these structures are possible from the viewpoint of the balance between *E*(L) and *E*(NL). It should be noted only that structure **2b** is more stable due to *E*(L) contribution, while **2c** is more stable due to *E*(NL) contribution, but $\Delta E(NL)>3\cdot\Delta E(L)$. So, in this case some factors of stabilization differ from expected steric and electrostatic differences. For compound **2** without perchlorate anion, the schematic energy profiles of *E*(L) and *E*(NL) are similar to the case of **2a**–**d**. However, for **2b′** and **2c′** the values of ΔE(L) and ΔE(NL) are of the same order. It allows us to suppose that **2c** is more stable than **2b** due to the effect of perchlorate anion on the cationic part.

In terms of the NBO theory, there are no bonds between anionic and cationic fragments in the studied structures. There are the multiply second-order interactions between the fragments with very small the stabilization energy *E*(2) with values close to zero. In structures **1a**–**d** the maximum of *E*(2) is 3.63 kcal mol^{-1}, whereas for **2a**–**d** the maximum of *E*(2) is 1.86 kcal mol^{-1}. It allows us to look in a new way at the questions posed earlier[23] about chemical bonds in similar compounds. We tend to associate the interactions between anionic and cationic fragments more with the electrostatic nature of the ionic parts than with interactions between atoms orbitals according the current level of calculations.

We assume that the difference in structure stabilization for compounds **1** and **2** with respect to the previously known spiropyrans is due to the presence of an extended conjugation chain in the molecule and different efficiency of conjugation for **1** and **2**. In order to qualitatively assess the effect of conjugation, the ESP charge redistribution in the isomeric structures during possible isomerization reactions was studied (see Online Supplementary Materials, Figures S1 and S2). The quantitative changes of atomic charges are given in Table S5. It was found that there was an equalization of ESP charges along the skeleton of the cationic fragment during passing from **1a** to **1d**. In case of compound **2**, the positive charge is initially distributed over the entire backbone, and its migration is combined with the location at several carbon atoms. The negative charge migrates far enough along cationic part, except for a case of oxygen atoms. The Mulliken and APT (Atomic Polar Tensor) charges have been also investigated. The problems of Mulliken charges such as basis choice sensitivity are well known. The calculations show that the pyran ring is broken and the charge of oxygen atom O(1′) changes its sign in compounds **1** and **2** (see Online Supplementary Materials, Scheme S1 and Table S5) with value sufficiently differ from zero, which contradicts the electronegativities of this atom. This may point out to the inadequacy of the Mulliken scheme in this case. Calculated APT charge of atom N(1) in structures **1a** and **2a** is negative that makes doubt in acceptance of this scheme for studied compounds also.

The geometry configuration of **1a** shows that a carbon bridge has the single-double-single bond pattern. This bridge remains intact during the hypothetical isomerization process of compound **1**. Also, after the opening of pyran ring the second bridge appears where the bonds transform to three resonance hybrid bonds. It based on a comparison of computed bond lengths (Table S7) with table values of characteristic bond lengths in free molecules.[24] The similar situation with the bonds of carbon bridges also takes place in compound **2**.

The qualitative geometry changes of the studied structures in the dependence on the presence of perchlorate anion are illustrated in Figures S3 and S4. It is shown that according to calculations (see Table S7), the distortion of the cationic moiety is more for **1c** and **1d** and it is caused by the interaction of this moiety and the perchlorate anion. The isomeric structures of compound **2** are more sustained for different geometric changes connected with anion effect. Compared to the XRD data, in the gas phase double bonds are elongated and single bonds are shortened (Table S6). Thus, the conjugation is more pronounced without environmental effects.

The qualitative effect of the perchlorate anion on **3c**–**4e** hyperbond in the studied isomeric structures (Figures S5 and S6) is based on NBO analysis (Table S8). So, despite the absence of bonds between anionic and cationic fragments in the studied structures, the perchlorate anion noticeably affects a position of hyperbonds in case of **1b** and **1b′**. In other cases, such effect is not so obvious.

This work was financially supported by the Russian Foundation for Basic Research (grant no. 20-03-00214A, B. S. Lukyanov), the Ministry of Science and Higher Education of the Russian Federation (State assignment in the field of scientific activity, Southern Federal University, no. 0852-2020-00-19, V. V. Koval and I. M. El-Sewify), as well as the Strategic Academic Leadership Program of the Southern Federal University (‘Priority 2030’, A. S. Kozlenko).

Online Supplementary Materials

Supplementary data associated with this article can be found in the online version at doi: 10.1016/j.mencom.2022.07.013.

References

1 R. Klajn, *Chem. Soc. Rev.*, 2014, **43**, 148.
2 B. L. Feringa, *Angew. Chem., Int. Ed.*, 2017, **56**, 11060.
3 W. A. Velema, M. J. Hansen, M. M. Lerch, A. J. M. Driessen, W. Szymanski and B. L. Feringa, *Bioconjugate Chem.*, 2015, **26**, 2592.
4 I. V. Ozhogin, P. V. Zolotukhin, V. V. Tkachev, A. D. Pugachev, A. S. Kozlenko, A. A. Belanova, S. M. Aldoshin and B. S. Lukyanov, *Russ. Chem. Bull.*, 2021, **70**, 1388.
5 I. V. Dorogan and V. I. Minkin, *Chem. Heterocycl. Compd.*, 2016, **52**, 730.
6 Y. Sheng, J. Leszczynski, A. A. Garcia, R. Rosario, D. Gust and J. Springer, *J. Phys. Chem. B*, 2004, **108**, 16233.
7 O. Kovalenko and M. Reguero, *Phys. Scr.*, 2020, **95**, 055402.
8 L. Kortekaas and W. R. Browne, *Chem. Soc. Rev.*, 2019, **48**, 3406.
9 M. Schulz-Senft, P. J. Gates, F. D. Sönnichsen and A. Staubitz, *Dyes Pigm.*, 2017, **136**, 292.
10 A. S. Kozlenko, N. I. Makarova, I. V. Ozhogin, A. D. Pugachev, M. B. Lukyanova, I. A. Rostovtseva, G. S. Borodkin, N. V. Stankevich, A. V. Metelitsa and B. S. Lukyanov, *Mendeleev Commun.*, 2021, **31**, 403.
11 A. D. Pugachev, M. B. Lukyanova, B. S. Lukyanov, I. V. Ozhogin, A. S. Kozlenko, V. V. Tkachev, P. B. Chepurnoi, G. V. Shilov, V. I. Minkin and S. M. Aldoshin, *Dokl. Chem.*, 2020, **492**, 76 (*Dokl. Ross. Akad. Nauk, Nauki Mater.*, 2020, **492**, 23).
12 V. V. Koval, A. S. Kozlenko, V. I. Minkin and B. S. Lukyanov, *Russ. J. Gen. Chem.*, 2021, **91**, 1150 (*Zh. Obshch. Khim.*, 2021, **91**, 977).
13 G. Cottone, R. Noto and G. La Manna, *Chem. Phys. Lett.*, 2004, **388**, 218.
14 M. B. Lukyanova, V. V. Tkachev, B. S. Lukyanov, A. D. Pugachev, I. V. Ozhogin, O. A. Komissarova, S. M. Aldoshin and V. I. Minkin, *J. Struct. Chem.*, 2018, **59**, 565.
15 M. J. Frisch, G. W. Trucks, H. B. Schlegel, G. E. Scuseria, M. A. Robb, J. R. Cheeseman, G. Scalmani, V. Barone, G. A. Petersson, H. Nakatsuji, X. Li, M. Caricato, A. V. Marenich, J. Bloino, B. G. Janesko, R. Gomperts, B. Mennucci, H. P. Hratchian, J. V. Ortiz, A. F. Izmaylov, J. L. Sonnenberg, D. Williams-Young, F. Ding, F. Lipparini, F. Egidi, J. Goings, B. Peng, A. Petrone, T. Henderson, D. Ranasinghe, V. G. Zakrzewski, J. Gao, N. Rega, G. Zheng, W. Liang, M. Hada, M. Ehara, K. Toyota, R. Fukuda, J. Hasegawa, M. Ishida, T. Nakajima, Y. Honda, O. Kitao, H. Nakai, T. Vreven, K. Throssell, J. A. Montgomery, Jr., J. E. Peralta, F. Ogliaro, M. J. Bearpark, J. J. Heyd, E. N. Brothers, K. N. Kudin, V. N. Staroverov, T. A. Keith, R. Kobayashi, J. Normand, K. Raghavachari, A. P. Rendell, J. C. Burant, S. S. Iyengar, J. Tomasi, M. Cossi, J. M. Millam, M. Klene, C. Adamo, R. Cammi, J. W. Ochterski, R. L. Martin, K. Morokuma, O. Farkas, J. B. Foresman and D. J. Fox, *Gaussian 16, Revision C.01*, Gaussian, Wallingford, CT, 2016.
16 A. D. Becke, *J. Chem. Phys.*, 1993, **98**, 5648.
17 R. Krishnan, J. S. Binkley, R. Seeger and J. A. Pople, *J. Chem. Phys.*, 1980, **72**, 650.

18 E. D. Glendening, J. K. Badenhoop, A. E. Reed, J. E. Carpenter, J. A. Bohmann, C. M. Morales, C. R. Landis and F. Weinhold, *NBO 6.0: Natural Bond Orbital Analysis Program*, Madison, WI, 2013, http://nbo6.chem.wisc.edu.
19 G. A. Zhurko, *Chemcraft – Graphical Program for Visualization of Quantum Chemistry Computations*, Ivanovo, Russia, 2005, https://chemcraftprog.com.
20 R. Dennington, T. A. Keith and J. M. Millam, *GaussView, Version 6.0*, Semichem, Shawnee Mission, KS, 2016.
21 J. Hobley and V. Malatesta, *Phys. Chem. Chem. Phys.*, 2000, **2**, 57.
22 G. Cottone, R. Noto and G. La Manna, *Molecules*, 2008, **13**, 1246.
23 S. M. Aldoshin, *Russ. Chem. Rev.*, 1990, **59**, 663 (*Usp. Khim*., 1990, **59**, 1144).
24 *CRC Handbook of Chemistry and Physics*, 84th edn., ed. D. R. Lide, CRC Press, Boca Raton, 2003.

Received: 10th February 2022; Com. 22/6804